

This document downloaded from
vulcanhammer.net vulcanhammer.info
Chet Aero Marine



Don't forget to visit our companion site
<http://www.vulcanhammer.org>

Use subject to the terms and conditions of the respective websites.

Estimating Load-Deflection Characteristics for the Shaft Resistance of Piles Using Hyperbolic Strain Softening

Don C. Warrington, PhD., P.E.
University of Tennessee at Chattanooga
Department of Mechanical Engineering

Hyperbolic soil modelling and strain softening have become better understood in recent years; however, their application to modelling load-deflection characteristics for the shaft of both bored and driven piles is in the early stages of development. This paper proposes a method that is based strictly on the strain-softening changes in shear modulus that is experienced to varying degrees around the pile shaft. A dimensionless method is proposed which can be transformed to a physical estimate using simple soil parameters.

Keywords: shaft resistance, driven piles, bored piles, strain softening, hyperbolic soil model

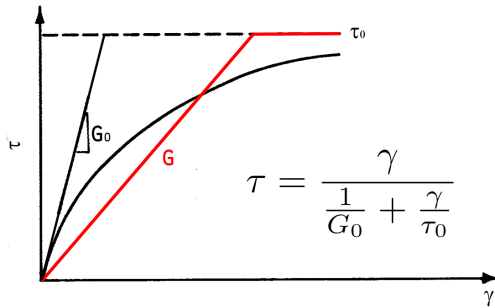


Figure 1. Hyperbolic Soil Model

Introduction

Although it does not apply to all soils, the hyperbolic model of stress-strain response is well established (Duncan and Chang (1970).) It is definitely a step forward from the elastic-purely plastic model (frequently with Mohr-Coulomb failure) that is used extensively in geotechnical engineering. Nevertheless relating the two is important, if for no other reason because some of the quantities we derive can best be understood if the two concepts are placed side-by-side. This can be shown by considering Figure 1, where the hyperbolic response is shown in black and the “equivalent” elastic-plastic response is shown in red.

We can see that, as shear strain γ increases, the effective shear modulus G the soil presents to the loading decreases. This shear modulus is generally referred to as a secant shear modulus, which is the case, but establishing which secant to draw for a given level of stress is not immediately obvious from the relationship shown in Figure 1.

The phenomenon shown in Figure 1 is referred to as strain softening, and has been the subject of extensive research over

the last thirty years or so. An important study (for clays at least) of this phenomenon, with an extensive database of soil tests, can be found in Vardanega and Bolton (2013), although other studies of this have been done, as documented in Warrington (2019).

One application of the effects of shear strain in geotechnical engineering is the response of the soil along the shaft surface for both driven and bored piles. Although the one-dimensional models commonly used give the impression of strictly surface interaction, this is misleading. The movement of the pile (upward or downward) also induces displacement in the surrounding soil which enters into the stress-strain response of the pile surface and thus the pile itself (Randolph and Wroth (1978).)

As the pile moves relative to the soil, shear stresses and strains are induced in the soil, both at the pile surface and away from the pile. As strain increases the effective shear modulus of the soil decreases, which in turn affects the load-deflection characteristics of the pile, and do so in a way that the modulus varies with the distance from the pile surface. Recent studies, such as Bateman and Crispin (2020), both document attempts to solve this problem in the past and explore new solutions.

The purpose of this paper is to present a solution to this problem which both incorporates a newer understanding of the phenomenon of strain softening and simplifies the solution to the problem.

Basic Theory

Strain-Softening in Soils

In general,

$$\gamma = \frac{\tau}{G} \quad (1)$$

That being the case, we define the reference strain as follows:

$$\gamma_0 = \frac{\tau_0}{G_0} \quad (2)$$

Normalising the results using this concept is crucial; Vardanega and Bolton (2013) go so far as to say the following:

It is clear...that the maximum shear modulus, (G_0), is successful as a normalizer for shear modulus data and that the commonly used surrogates are not acceptable. It follows that (G_0) should ideally be estimated or measured when studies of soil stiffness degradation are undertaken.

From this we can define

$$\mu = \frac{G}{G_0} \quad (3)$$

We can also normalise the shear strain and define the shear strain ratio as

$$\aleph = \frac{\gamma}{\gamma_0} \quad (4)$$

Combining Equations 2 and 4, we have

$$\frac{\gamma}{\aleph} = \frac{\tau_0}{G_0} \quad (5)$$

or

$$\gamma = \frac{\aleph \tau_0}{G_0} \quad (6)$$

Substituting Equation 3 into Equation 1,

$$\gamma = \frac{\tau}{\mu G_0} \quad (7)$$

We then substitute Equation 2 to yield

$$\frac{\aleph \tau_0}{G_0} = \frac{\tau}{\mu G_0} \quad (8)$$

or

$$\frac{\tau}{\tau_0} = \mu \aleph \quad (9)$$

The strain-softening characteristic shown in Equation 3 can be described by the general relationship

$$\mu = \frac{\beta}{\beta + \aleph^\alpha} \quad (10)$$

and thus

$$\frac{\tau}{\tau_0} = \frac{\aleph \beta}{\beta + \aleph^\alpha} \quad (11)$$

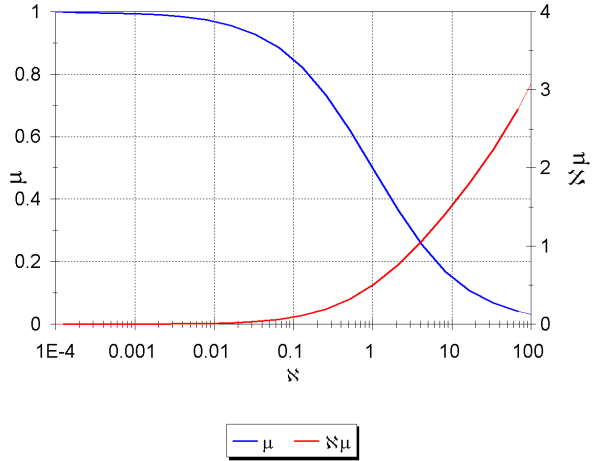


Figure 2. Softening Coefficient vs. Normalized Shear Strain (adapted in part from Vardanega and Bolton (2013))

To solve for \aleph and μ is most easily done using Newton's Method, as these functions are continuous and differentiable. As always the starting point is the most difficult part; our experience lead to using $\aleph = 0$ for this purpose.

It is now possible (assuming some values for α and β) to construct a plot of μ and $\frac{\tau}{\tau_0}$ as a function of \aleph , and this is done (using Equations 9, 10 and 11) in Figure 2.

It is worth noting that there are valid values of $\frac{\tau}{\tau_0} = \mu \aleph > 1$.

Shaft Resistance Soil Stresses and Strains

The shear stress due to the shaft resistance of the soil for any distance r_2 from the centreline of the pile can be shown to be (Randolph and Wroth (1978))

$$\tau_n = \tau_1 \frac{r_1}{r_n} \quad (12)$$

This is strictly an expression of static equilibrium; it is not a function of the elasticity (or lack thereof) of the soil, or changes in the shear modulus of the soil as the distance increases from the pile surface.

The shear strain at the pile surface is, from Equation 7,

$$\gamma_1 = \frac{\tau_1}{\mu_1 G_0} \quad (13)$$

The relationship between the shear stress at the pile surface and the maximum shear stress, from Equation 11,

$$\frac{\tau_1}{\tau_0} = \frac{\aleph_1 \beta}{\beta + \aleph_1^\alpha} \quad (14)$$

and μ_1 can be computed from Equation 10.

The strain at any point beyond the surface of the pile is given by

$$\gamma_n = \frac{\tau_n}{\mu_n G_0} \quad (15)$$

where τ_n is computed from Equation 12 and

$$\frac{\tau_n}{\tau_0} = \frac{\aleph_n \beta}{\beta + \aleph_n^\alpha} \quad (16)$$

where we solve first for \aleph_n and then compute μ_n using Equation 10. Since, from Equation 10, the value of μ_n will vary, the inhomogeneity of the soil due to shear softening is included in the model.

Deflection of the Pile Shaft

The deflection of the pile shaft not only takes place at the surface of the pile; it takes place in the surrounding soil, according to the following (Randolph and Wroth (1978)):

$$w_s = \frac{\tau_1 r_1}{G} \int_{r_1}^{\infty} \frac{dr}{r} \quad (17)$$

This formulation suffers from two weaknesses. The first is that, at the upper limit, it is unbounded. It is thus necessary to use a ‘‘magical radius’’ (Warrington (2019).) The second is that Equation 17 assumes a constant value of G , which is invalid, if for no other reason than for strain softening. Modifying this formulation for these two weaknesses yields

$$w_s = \tau_1 r_1 \int_{r_1}^{r_m} \frac{dr}{G(r)r} \quad (18)$$

The magical radius can be expressed dimensionlessly as

$$\hat{r}_m = \frac{r_m}{r_1} \quad (19)$$

An expression of $G(r)$ can be obtained by applying Equations 3 and 12; however, integrating this in closed form is difficult because of the nature of Equation 11. A simpler way is to consider that the integration can be divided up into rings of inner radius r_n and outer radius r_{n+1} and obtain the same result:

$$w_s = \tau_1 r_1 \sum_{n=1}^k \int_{r_n}^{r_{n+1}} \frac{dr}{\mu_n G_0 r} \quad (20)$$

where n is the number of rings necessary to achieve the magical radius. This will vary both with the magical radius and how the rings are divided. Integrating in this fashion yields

$$w_s = \tau_1 r_1 \sum_{n=1}^k \frac{\ln(r_{n+1}) - \ln(r_n)}{\mu_{n \rightarrow n+1} G_0} \quad (21)$$

If we define

$$\hat{r}_{n+1} = \frac{r_{n+1}}{r_1} \quad (22)$$

and

$$\hat{r}_n = \frac{r_n}{r_1} \quad (23)$$

and make other substitutions, we can define a dimensionless shaft deflection

$$\hat{w}_s = \aleph_1 \mu_1 \frac{\ln(\hat{r}_{n+1}) - \ln(\hat{r}_n)}{\mu_n} = \frac{G_0 w_s}{\tau_0 r_1} \quad (24)$$

which can be rearranged thus

$$w_s = \frac{\tau_0 r_1}{G_0} \hat{w}_s = \gamma_0 r_1 \hat{w}_s \quad (25)$$

Thus the dimensionless shaft deflection \hat{w}_s and the actual shaft deflection w_s can be related by basic soil properties and parameters at the pile surface.

Solving for Dimensionless Displacement

Outline of the Solution

The procedure for determining the dimensionless deflection of a portion of a pile shaft as a function of pile surface shear stress using this theory is as follows:

1. Establish a range of values of $\frac{\tau_1}{\tau_0}$ to analyse. For our purposes $0.05 \leq \frac{\tau_1}{\tau_0} \leq 0.95$. The zero stress point should induce no deflection in the pile and thus it is trivial. At the other end, looking at Figure 1, the value τ_0 is in principle the shear stress of the soil at failure. It is reasonable to assume that the pile-soil interface will fail at a different point than the soil itself, most likely at a lower shear stress, beyond which point the pile will move without further increase in soil stress.

2. It is necessary to assume values for α and β . For our purposes we will assume that $\alpha = 0.75$ and $\beta = 1$. This issue is discussed in Warrington (2019).

3. For each value of $\frac{\tau_1}{\tau_0}$ under consideration, first determine the value of \aleph_1 and μ_1 using Equations 14 and 10 respectively. This is done by applying Newton’s Method to Equation 14 and solving for \aleph_1 and thus μ_1 .

4. Assume a magical radius ratio \hat{r}_m . For this study $\hat{r}_m = 100$. The value of the magical radius is discussed in Warrington (2019).

5. Divide this region into small increments, each with endpoints $n, n + 1, n + 2, \dots$. Each endpoint has a radius ratio computed by Equations 22 and 23. An exponential method was used to divide the region into radial segments, which is different from that of Warrington (2016).

6. For each endpoint determine the stress ratio to the reference stress using Equation 12.

7. Again using Newton’s Method, determine \aleph_n and μ_n at each endpoint.

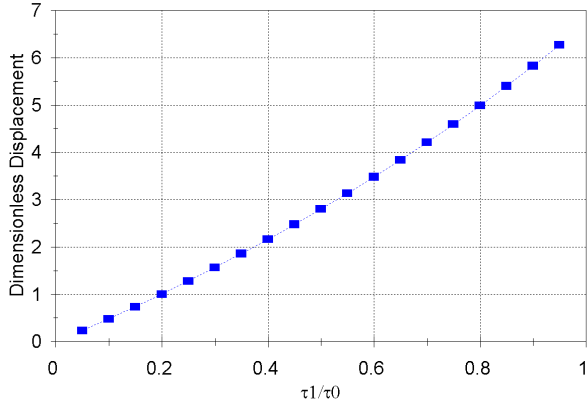


Figure 3. Dimensionless Displacement of Pile vs. Shear Stress Ratio

8. For each segment, estimate the average value of $\mu_{n \rightarrow n+1}$ as the average of the two values at the endpoints.

9. Estimate the dimensionless deflection for each segment using Equation 24.

10. Sum up these segmental dimensionless deflections for a total \hat{w}_s for a given value of $\frac{\tau_1}{\tau_0}$.

11. Repeat this process for all values of $\frac{\tau_1}{\tau_0}$ under consideration.

Results of the Solution

A routine was written to perform the solution. A summary of the results of this for the total dimensionless displacement \hat{w}_s is shown in Figure 3.

The results are slightly curved; a second-order correlation is fairly exact. However, a linear correlation (forcing the line through the origin) gives an good rendering of the results as

$$\hat{w}_s = 6.11 \frac{\tau_1}{\tau_0} \quad (26)$$

In a qualitative sense, this justifies the use of a purely elastic response of the soil to deflection before the bond between the pile and soil fails, as is generally done with t-z types of models (static and dynamic.) This can then be applied to Equation 25 of obtain the estimated deflection at a point along the shaft for a given applied shear stress.

The results can be seen in more detail if the displacements are plotted as a function of radius ratio from the pile surface to the magical radius. This is shown for some of the values of $\frac{\tau_1}{\tau_0}$ in Figure 4.

The markers show the midpoints of the radial segments the soil around the pile is divided into. It is easy to see the spacing increases with increasing radius ratio. The graph is drawn assuming that the displacement is zero at the magical radius; however, for the larger deflections it is also easy to see that the slope of the line (shear strain) is not quite zero at the magical radius. Determining the magical radius at which

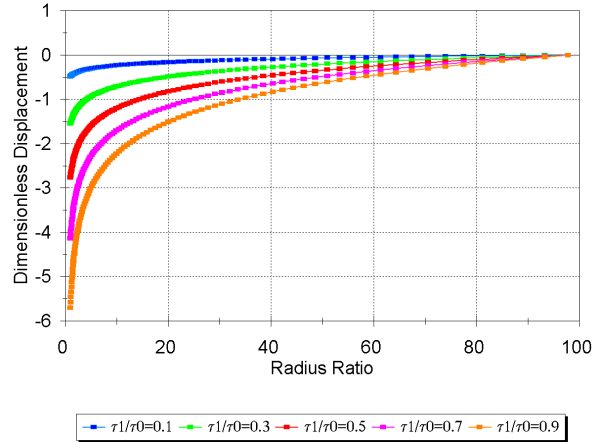


Figure 4. Soil Deflections as a Function of Radius Ratio

the soil becomes “insignificant” to pile displacements has been a major challenge since the concept was first set forth by Cooke (1974).

Notes on the Solution

1. The solution as presented here does not deal with physical soil parameters such as γ_0 , G_0 , or τ_0 . Such are beyond the scope of the study. It was necessary to assume values of α and β to obtain some kind of solution, although values of these (especially α) vary with soil and other aspects of the theory.

2. Although it is tempting to assume that τ_0 is the shear failure stress of the soil, putting this together with the other two parameters of Equation 2 may yield discrepancies. The relationship between these parameters and, say, Mohr-Coulomb parameters such as c_u and ϕ is something that needs further study.

3. The solution is, strictly speaking, only valid for rigid piles and soils with uniform soil properties along the shaft. However, it can be applied to more realistic scenarios if a) the soil is divided into layers with uniform properties and b) the response is considered on a layer-by-layer basis with provision for the axial flexibility of the pile. The results shown in Figure 3 give promise to the idea that these results can be applied to the elastic-purely plastic models that are prevalent with common t-z modelling schemes.

4. The solution assumes that the only source of alteration of the soil shear modulus is due to stresses induced by pile movement. With bored piles this may be reasonable; with driven piles, cavity expansion effects may alter this solution, perhaps in a time-dependent way.

5. The formulation here implicitly assumes a static loading the pile. With dynamic loading, other factors may be necessary to consider.

Conclusion

A simple method was developed to include the effects of strain-softening around driven piles due to shear stresses along the shaft. The method focuses on the reduction of the shear modulus to the exclusion of other parameters. For a more practical implementation the parameters necessary to transform the dimensionless results to actual physical ones need proper quantification.

Nomenclature

α	Parameter for strain-softening coefficient
β	Parameter for strain-softening coefficient
\aleph	Normalised Reference Strain
\aleph_1	Normalised Reference Strain at pile surface
\aleph_n	Normalised Reference Strain at a point away from the pile surface
γ	Shear Strain
γ_0	Reference Shear Strain
γ_1	Shear Strain at the Pile Surface
γ_n	Shear Strain at a point n from the pile surface
\hat{r}_m	Dimensionless Magical Radius
\hat{r}_{n+1}	Dimensionless Radius Ratio beyond \hat{r}_m
\hat{w}_s	Normalized Pile Displacement
μ	Hyperbolic strain softening coefficient
μ_1	Strain Softening Coefficient at the Pile Surface
μ_n	Strain Softening Coefficient at a point n from the pile surface
$\mu_{n \rightarrow n+1}$	Averaged/Homogenised Strain Softening Coefficient in an annular ring
ϕ	Internal Friction Angle, radians
τ	Shear Stress, kPa
τ_0	Reference Shear Stress, kPa
τ_1	Shear Stress at the Pile Surface, kPa
τ_n	Shear Stress at a point n away from the pile, kPa

c_u	Cohesion, kPa
G	Shear Modulus of Elasticity, kPa
G_0	Small-Strain Shear Modulus of Elasticity, kPa
k	Number of Rings for Computation of Dimensionless Displacement
r	Radius From Pile Center, m
r_1	Radius of the Pile, m
r_n	Radius from pile centreline, m
r_m	Magical Radius, m
r_{n+1}	Radius from pile centreline beyond r_n , m
w_s	Deflection at Pile Surface, m

References

- Bateman, A., & Crispin, J. (2020, October). Theoretical “t-z” curves for piles in radially inhomogeneous soil. *DFI Journal: The Journal of the Deep Foundations Institute*, 14(1). doi: 10.37308/DFIJnl.20190930.210
- Cooke, R. (1974, December). The settlement of friction pile foundations. *Conference on Tall Buildings, Peninsular Malaysia Conference Organizing Committee*, 7–19.
- Duncan, J. M., & Chang, C.-Y. (1970, September). Nonlinear analysis of stress and strain in soils. *Journal of the Soil Mechanics and Foundations Division*, 96(SM5), 1629–1653.
- Randolph, M., & Wroth, C. (1978, December). Analysis of deformation of vertically loaded piles. *Journal of the Geotechnical Engineering Division*, 104(GT12).
- Vardanega, P., & Bolton, M. (2013, September). Stiffness of clays and silts: Normalizing shear modulus and shear strain. *Journal of Geotechnical and Geoenvironmental Engineerings*, 139, 1575–1589.
- Warrington, D. C. (2016). *Improved methods for forward and inverse solution of the wave equation for piles* (Unpublished doctoral dissertation). University of Tennessee at Chattanooga, Chattanooga, TN.
- Warrington, D. C. (2019, July). *Application of the stady program to analyze piles driven into sand* (Tech. Rep.). doi: 10.13140/RG.2.2.22311.09125/1